A Robust Control Strategy for Sensorless Under-Tendon-Driven Prosthetic Hands

Julio Fajardo[1,2], Diego Cardona[1], Guillermo Maldonado[1], Victor Ferman[2] and Eric Rohmer[2]

***Abstract*—One of the most significant reasons for the abandonment of multifunctional prosthetic hands is the poor functionality they may yield. This is directly related to the controllability of the wrench exerted by the fingers, as well as the accurate positioning and decent responsiveness the prosthesis may provide while interacting with different objects during activities of daily living. Typical approaches to solve this problem involve using complex array sensors, which increase the artificial limb's price, size, and weight. This work proposes a method to achieve this goal without complex hardware by using a sensorless hybrid control strategy based on an on-off controller to control the fingertips' force on the closing process and a robust position controller on the opening process. Both controllers work in tandem with a robust full-state observer to estimate the motor's shaft's angular position that closes and drives back the fingers to the rest position. This strategy was validated on an under-tendon-driven upper-limb prosthetic device showing successful results.**

***Index Terms*—Upper-limb prosthesis, sensorless system.**

I. Introduction

Even with the known advantages of electric prostheses over the body-powered ones, the rejection rate for the bionic alternative lies around 23% for adults, which, in most cases, is due to cost, weight, maintainability, and functionality [1], [2]. Since the control strategy directly affects the use of hardware in the prosthetic device and its performance, all of the aspects mentioned above can be improved using an efficient controller/observer approach implemented on a compact, lightweight, and affordable embedded system.

Generally, sensorless control systems tend to either implement open-loop or observer techniques. The first one requires the user to regulate the speed and force exerted by the prosthesis according to the behavior noticed by them [3]; this shows an affordable, low-maintenance, and simple option for achieving the desired purpose. However, a proportional controller is not very efficient since the overshoot is increased, and it is difficult for the user to adjust its parameters only through visual stimuli. That is why sensor-feedback is often referred to when implementing controllers; typical approaches to close the position or force control loops of prosthetic hands involve using potentiometers or quadrature encoders and tactile/pressure sensors respectively [4]–[7]. Often combining integral control with different methods to improve its overall performance, like multiple feedback loops and anti-windup schemes [3], [8]. These techniques increase the price and, in some cases, the device's size, leading patients to settle for lightweight aesthetic prosthesis or to use none at all [9]. The other alternative relies on using a state observer, which is commonly implemented by measuring the current or voltage demanded by the actuators to estimate the full state of the system. In contrast to previous approaches, this can even allow for the system to eliminate the use of sensors on the prosthetic device, reduce its size and cost, and facilitate its repairability and maintenance (as the system is simplified) [10]. Sensorless observers tend to be divided into two different approaches. First, the ones that estimate the angular speed of the motor's shaft based on the ripple component of the signal [11], [12]. On the other hand, the ones that can estimate their states based on the dynamic linear model of brushed DC motors. [13], [14]. Other systems employ a stochastic dynamical system to improve the estimation of the full state, providing robustness to the exogenous disturbances that may arise from the sensor and the process itself; some of them are the Kalman (KF), extended Kalman (EKF), and the particle (PF) filters [15]–[17]. The main issue with such approaches is that the resulting errors need to be modeled as Gaussian, causing practical application issues. However, $\mathcal{H}_\infty$-based, energy-bounded observers may obtain similar results with a convergent solution without an idealized model of the noise [18].

In this work, a hybrid robust control strategy is presented to implement on the embedded system of a sensorless upper-limb prosthesis. For that reason, an approximated model of the system was employed to reduce the computational load on the controller. Besides, this strategy works together with an $\mathcal{H}_\infty$ observer to estimate the states of the motor that is part of the under-tendon-driven (UTD) system that drives each finger of the Galileo Hand, an anthropomorphic, affordable upper-limb prosthesis [19], [20].

The rest of this paper is structured as follows: Section II elaborates on the hardware used to run the tests and the dynamics of the UTD machine. Section III indicates the problems involved in designing a low-level observer/controller architecture. Section IV elaborates on the discrete-time $\mathcal{H}_\infty$ observer and Section V delves into the overall control strategy implemented. The experimental results and conclusions are presented in Sections VI and VII, respectively.

[1] Author is with Turing Research Laboratory, FISICC, Galileo University, Guatemala City, Guatemala. guiller@galileo.edu

[2] Author is with the Department of Computer Engineering and Industrial Automation, FEEC, UNICAMP, 13083-852 Campinas, SP, Brazil. {julioef,vferman,eric}@dca.fee.unicamp.br

II. Mechanical System

A. Galileo Hand

The Galileo Hand (illustrated in Fig. 1), is an open-source and UTD myoelectric upper-limb prosthesis for unilateral transradial amputees [19], [20]. Three phalanges conform its digits: distal, proximal, and middle; as well as three joints: distal and proximal interphalangeal (DIP and PIP) and the metacarpophalangeal (MCP) one (illustrated in Fig. 2), ergo, every finger has 3 degrees of freedom (DOF) [20]. A single brushed DC motor actuates every limb with a gear ratio of 250:1 and an output torque of around $0.42Nm$, which results in one degree of actuation (DOA) for each digit. The thumb mechanism functions differently, as it possesses 2 DOA: one for the flexion/extension and another for the abduction/adduction movements [20].

B. The Under-tendon-driven Machine

Each finger's flexion and extension process is achieved by operating two tendons: an active and a passive one. The first one is a waxed nylon cord actuated by its corresponding motor, which closes the digit. The second one consists of a round, surgical-grade elastic that springs the finger back open.

This results in a positive tensile force, f_{ta}, when the motor coils the string; and a passive one, f_{te}, which is uniquely dependant on the deflection of the joints; opposing itself to its active counterpart [20], [21]. So, the following relationship for the generalized coordinates, q, and the motor angle vector, θ, can be obtained

$$\mathbf{q} = \mathbf{J}_j^{+} \left[\boldsymbol{l} - \boldsymbol{l}_0 - \mathbf{J}_a \boldsymbol{\theta} \right] + \mathbf{q}_0 \tag{1}$$

such that $\boldsymbol{l} = \begin{bmatrix} l_a & l_e \end{bmatrix}^T$ is the deflection of the active, l_a, and the passive, l_e, tendons; $\boldsymbol{l}_0 = \begin{bmatrix} 0 & l_{e0} \end{bmatrix}^T$ and $\mathbf{q}_0$, the initial expansion of the tendons and angular displacement of the joints, respectively; and $\mathbf{J}_a$, the Jacobian matrix related to the actuator. In addition to that, $\left(\mathbf{J}_j^T\right)^{+}$ is the Moore-Penrose pseudoinverse of the transposed Jacobian matrix J_j composed by the active and passive tendons as $\mathbf{J}_j = \begin{bmatrix} \mathbf{J}_{ja} & \mathbf{J}_{je} \end{bmatrix}^T$, which results in the following expression (for a two-tendon, $L = 2$, and three-jointed, $N = 3$, model)

$$\mathbf{J}_j = \begin{bmatrix} r & r & r \\ -r & -r & -r \end{bmatrix} \tag{2}$$

considering that r is the radius of the joint's pulleys.

Similarly, the following expression can be utilized to determine the torque exerted by each joint, $\boldsymbol{\tau} \in \mathbb{R}^N$

$$\boldsymbol{\tau} = -\mathbf{J}_j^T \boldsymbol{f}_t \tag{3}$$

where the tensile force, $\boldsymbol{f}_t \in \mathbb{R}^L \ni \boldsymbol{f}_t = \begin{bmatrix} f_{ta} & f_{te} \end{bmatrix}^T$, can be determined with the following equation

$$\boldsymbol{f}_t = \boldsymbol{f}_b - \left(\mathbf{J}_j^T\right)^{+} \boldsymbol{\tau} \tag{4}$$

with $\boldsymbol{f}_b \in \mathbb{R}^L$ being a bias force vector that prevents the tendons from loosening and does not have an impact on $\boldsymbol{\tau}$; it is defined as follows

$$\boldsymbol{f}_b = \mathbf{A}\boldsymbol{\xi}\,, \qquad \mathbf{A} = \left[\mathbf{I}_L - (\mathbf{J}_j^T)^{+}\mathbf{J}_j^T\right] \tag{5}$$

such that $\boldsymbol{\xi}$ is a compatible dimensional vector with $\mathbf{A}$ and $\mathbf{I}_L$ is the identity matrix of size L.

Thus, since a positive initial expansion of the passive tendon, l_{e0}, to prevent the tendons from loosening, is considered for each finger, $\boldsymbol{f}_b > 0$, and $\operatorname{rank}(\mathbf{J}_j) = 1 < \mathbf{N}$, this results in a UTD mechanism described by the following dynamic system

$$\mathbf{M}(\mathbf{q})\,\ddot{\mathbf{q}} + \mathbf{C}(\mathbf{q}, \dot{\mathbf{q}})\,\dot{\mathbf{q}} + \mathbf{G}_g(\mathbf{q}) + \mathbf{J}_j^T \boldsymbol{f}_t = 0 \tag{6}$$

$$J_m \ddot{\theta} + b\dot{\theta} + r_p f_{ta} = \tau_m \tag{7}$$

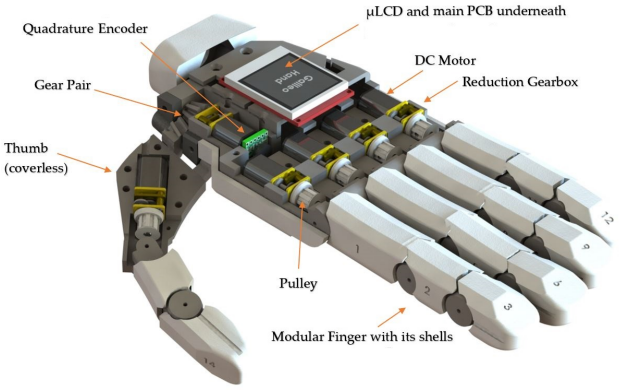

Fig. 1. Mechanical design of the Galileo Hand.

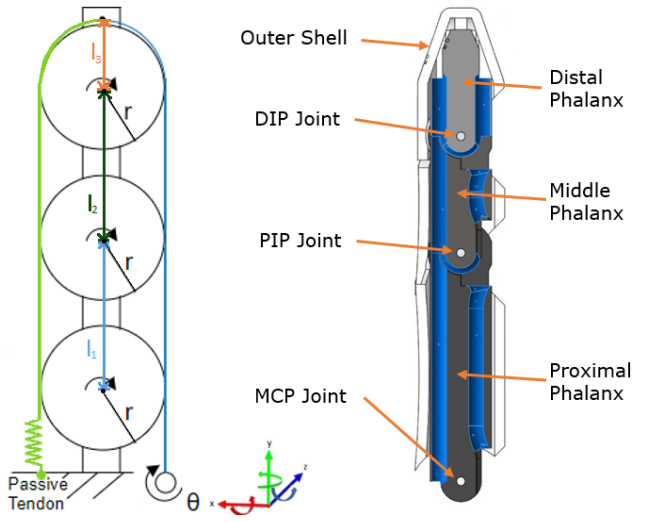

Fig. 2. UTD system, where r is the pulley's radius; θ, the gearhead shaft's angular position; and l_1, l_2 and l_3 indicate the length of each phalanx.

where $\mathbf{M}(\mathbf{q})$ is the inertia matrix of the finger, $\mathbf{C}(\mathbf{q}, \dot{\mathbf{q}})$ is the Coriolis matrix and $\mathbf{G}_g(\mathbf{q})$ is the gravity load matrix. Additionally, J_m and b are the gearhead's moment of inertia and friction coefficient, correspondingly; τ_m, the torque exerted by the motor gearhead's shaft; and r_p, the radius of the pulley mounted on it [21].

III. Problem Statement

To control the force exerted by the fingers and the position of the gearhead's shaft that drives the fingers on the artificial hand, one must be able to determine both of those parameters for all points in time. Thereby, one can regulate them to the desired value and operate the actuators on the prosthesis accordingly. On the other hand, the Eq. (6) shows that the finger's dynamic behavior is non-linear, mainly due to the nature of its terms (due to the mass matrix, centripetal, and Coriolis forces). Thus, it is difficult to estimate the full state of the coupled system of differential equations, (6)-(7).

In this way, an approximate linear model was used instead, considering the dynamic equations of motion of the finger as a mass-spring system. Since the passive tendon opposes the flexion movement but favors the extension one, its behavior is similar to that of a UTD machine. Therefore, it simplifies the computational load since it is unnecessary to linearize the model, allowing the implementation of this control strategy on the microcontroller unit (MCU) used on the prosthetic device.

This mechanism does not have a mechanical limit to stop the extension movement, unlike the flexion, whose movement is limited when the finger is entirely closed or when it comes into contact with another object. This causes the motor to continue actuating the digit and flexing it again (as the pulley coils the string in the opposite direction), making it difficult to control the extension movement without using a position sensor on the gearhead shaft. This could be fixed by measuring the time the finger requires to close and calculating the extension time (since they are not equal, as the passive tendon opposes itself to the coiling mechanism, but favors its counterpart) [19], [20]. However, this method is unreliable, as any possible disturbance while acting may provide an offset in that angular position.

On the other hand, if the fingertip position is known and related to the motor angle vector θ, one can close the fingers without any of the problems mentioned previously. Hence, the purpose of implementing a robust observer is to determine the angular displacement and velocity of the gearhead's shaft only, leading to not requiring an exact result for the generalized coordinates $\mathbf{q}$. However, the estimated state is useful to get an approximation of this parameter as well as the joints' torque, $\boldsymbol{\tau}$ by employing Eqs. (1) and (6).

Considering i_a as the armature current demanded by the DC motors, G_r as the gear ratio, k_t as the motor's constant, and η as the gearhead's efficiency, τ_m can be obtained with the following expression:

$$\tau_m = \eta G_r k_t i_a \tag{8}$$

Thus, the continuous-time state-space model for brushed DC motors results in:

$$\dot{\mathbf{x}} = \begin{bmatrix} 0 & 1 & 0 \\ -\frac{k_e r_p^2}{J_m} & -\frac{b}{J_m} & \frac{k_t}{J_m} \\ 0 & -\frac{k_t}{L_a} & -\frac{R_a}{L_a} \end{bmatrix} \mathbf{x} + \begin{bmatrix} 0 \\ 0 \\ \frac{1}{L_a} \end{bmatrix} u \tag{9}$$

$$\mathbf{y} = \begin{bmatrix} 0 & 0 & 1 \end{bmatrix} \mathbf{x} \tag{10}$$

where $\mathbf{x} = \begin{bmatrix} \theta & \dot{\theta} & i_a \end{bmatrix}^T$, with θ and $\dot{\theta}$ being the gearhead's angular position and velocity, respectively; R_a is the armature's resistance, L_a is the motor's inductance, k_e is the elastic constant of the passive tendon, u is the applied voltage, and $\mathbf{y}$ is the measured output.

IV. Discrete-time $\mathcal{H}_\infty$ Full-State Observer

A discretization of the simplified system is required for designing the control strategy, so considering the noise components and a sampling time k, it results as follows

$$\mathbf{x}_{k+1} = \mathbf{A}\mathbf{x}_k + \mathbf{B}_1\mathbf{u}_k + \mathbf{B}_2\mathbf{w}_k \tag{11}$$

$$\mathbf{y}_k = \mathbf{C}\mathbf{x}_k + \mathbf{D}_1\mathbf{v}_k + \mathbf{D}_2\mathbf{w}_k \tag{12}$$

where $\mathbf{x}_k \in \mathbb{R}^n$, $\mathbf{u}_k \in \mathbb{R}^p$, $\mathbf{y}_k \in \mathbb{R}^q$, $\mathbf{w}_k \in \mathbb{R}^s$ and $\mathbf{v}_k \in \mathbb{R}^t$ are the state, control input, measured output, process and measurement noise vectors, correspondingly. Moreover, $\mathbf{A} \in \mathbb{R}^{n\times n}$, $\mathbf{B}_1 \in \mathbb{R}^{n\times p}$, $\mathbf{B}_2 \in \mathbb{R}^{n\times s}$, $\mathbf{C} \in \mathbb{R}^{q\times n}$, $\mathbf{D}_1 \in \mathbb{R}^{q\times t}$ and $\mathbf{D}_2 \in \mathbb{R}^{q\times s}$ are the process, input control and input process noise, measured output, as well as the output process and output sensor noise matrices, respectively.

So, by considering a general noise vector, $\tilde{\mathbf{w}}_k = [\mathbf{w}_k \ \mathbf{v}_k]^T$, an observer-based filter can be described by

$$\hat{\mathbf{x}}_{k+1} = \mathbf{A}\hat{\mathbf{x}}_k + \mathbf{B}_1\mathbf{u}_k - \mathbf{L}(\mathbf{y}_k - \hat{\mathbf{y}}_k) \tag{13}$$

where $\hat{\mathbf{x}}_k \in \mathbb{R}^n$ is the estimated state; $\hat{\mathbf{y}}_k \in \mathbb{R}^n$ the estimated output; and $\mathbf{L}$, the observer gain.

Therefore, based on what is presented in work [18], an observer that meets robust requirements, where the error filtering, $\mathbf{e}_k$, has to satisfy that $\|\mathbf{e}_k\|_2 \leq \gamma(\|\mathbf{w}_k\|_2 + \|\mathbf{v}_k\|_2)$, with the robustness level $\gamma \in \mathbb{R} \ni \gamma > 0$, can be successfully characterized if a solution to the following convex optimization problem can be found

$$\min_{\mathbf{Z},\mathbf{G},\mathbf{P}=\mathbf{P}^T>0} \gamma \tag{14}$$

subjected to the following linear matrix inequality (LMI)

$$\begin{bmatrix} \mathbf{P} & \mathbf{A}^T\mathbf{G} + \mathbf{C}^T\mathbf{Z}^T & \mathbf{0}_{n\times s} & \mathbf{0}_{n\times s} & \mathbf{C}^T \\ \star & \mathbf{G} + \mathbf{G}^T - \mathbf{P} & \mathbf{G}^T\mathbf{B}_2 + \mathbf{Z}\mathbf{D}_2 & \mathbf{Z}\mathbf{D}_1 & \mathbf{0}_{n\times q} \\ \star & \star & \mathbf{I}_s & \mathbf{0}_{s\times s} & \mathbf{D}_2^T \\ \star & \star & \star & \mathbf{I}_s & \mathbf{D}_1^T \\ \star & \star & \star & \star & \gamma^2\mathbf{I}_q \end{bmatrix} > \mathbf{0} \tag{15}$$

where the matrices $\mathbf{Z} \in \mathbb{R}^{n\times q}$ and $\mathbf{P}$ are the variables of the problem and $\mathbf{G} \in \mathbb{R}^{n\times n}$ a slack variable [22]. Since $\mathbf{G}+\mathbf{G}^T > \mathbf{P} > 0$, $\mathbf{G}$ is non-singular, resulting in $\mathbf{L}$ being able to be recovered by evaluating the equation mentioned underneath [22].

$$\mathbf{L} = (\mathbf{G}^T)^{-1}\mathbf{Z} \tag{16}$$

V. Control Strategy

Once the UTD system's full state is known, one can input the estimated state to a controller to regulate or limit the values of specific parameters, like the fingertip force and joint torques. For this, one can solve the forward and velocity kinematics of the finger (3-link planar arm) to know their values for every instant in time by employing the Eqs. (1), (6), as well as the following expression.

$$\boldsymbol{f}_{tip} = (\mathbf{J}(\mathbf{q})^T)^{+}\boldsymbol{\tau} \tag{17}$$

where $\boldsymbol{f}_{tip}$ is the force exerted by the fingertip, $\mathbf{J}(\mathbf{q})$ is the space Jacobian matrix in 2D that relates the twist of the fingertip $\mathcal{V}_{tip}$ with the generalized velocities $\dot{\mathbf{q}}$, as follows

$$\mathcal{V}_{tip} = \mathbf{J}(\mathbf{q})\dot{\mathbf{q}} \tag{18}$$

At a high level, different techniques can be used to interpret the user's intent gathered by a user-prosthesis interface (UPI), where the vast majority are based on electromyography (EMG) as an acquisition method. In this way, based on what the UPI has interpreted, the system decides which fingers have to be flexed and which not to achieve a desired grip or gesture.

Therefore, considering that the fingers on the artificial hand behave similar to a non-backdrivable system, the on-off controller was designed to achieve the flexion movements with the necessary force $\boldsymbol{f}_{tip}$ to hold different objects. In contrast, the robust full state observer is utilized to estimate the angular displacement θ of the gearhead shaft for each motor (no quadrature encoders are employed) [18]. This estimation is used to have the necessary feedback to perform the extension movement using a robust feedback controller that drives back the finger to its initial position θ_0.

At a low level, each finger functions with an individual hybrid control strategy (on-off controller for the flexion process, robust feedback controller for the extension process), except for the thumb, which possesses, additionally, a quadrature encoder to implement a PI position controller for its rotation.

A. On-off Controller

Since the armature current i_a of each DC motor is the only feedback signal measured from the system, a simple force on-off controller is implemented to perform the flexion process. In this manner, by constantly monitoring the armature current i_a from each DC motor and, used together with the robust observer described in Sec. 4, one can easily related with the fingertip force $\boldsymbol{f}_{tip}$ using expressions (1), (6), (7), (8) and (17). Thus, the prosthesis can perform different predefined grips, ensuring that these are stable since the system limits the force exerted by each finger, as illustrated in the Finite State Machine in Fig. 3.

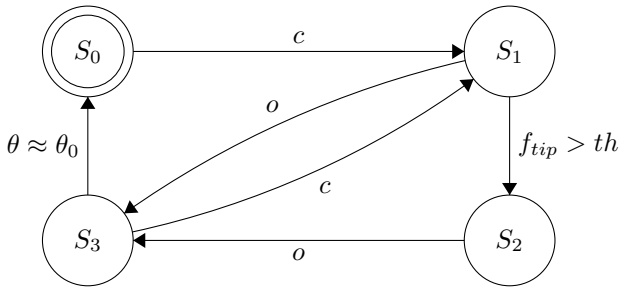

Fig. 3. FSM demonstrating the opening/closing behaviour of each finger.

The system starts with the finger fully extended in a rest position ("open", at $\theta = \theta_0$), modeled by the state S_0. The transition to S_1 happens when the high-level controller (HLC) sends the command to flex the finger, c. This drives the motor and causes the finger to start closing. While in this state, the estimated fingertip force $\boldsymbol{f}_{tip}$ is continuously determined and, when a predefined threshold, th, is exceeded, the transition to S_2 happens. This parameter may differ for each finger, as each one has a different size and, consequently, discrepant mechanical factors, so the calibration process was carried out experimentally.

At this point, the finger is considered completely closed or could be one or more of its phalanges touching the surface of an object. Then, it will begin to open if and only if the o command is issued by the HLC, as shown by the transition from S_2 to S_3. The alteration in state from S_3 to S_0 happens after the angular displacement, θ is approximated to its initial value $\theta_0 = 0$ (driven by the feedback controller described in Sec. V-B). This strategy was adopted since the passive tendon (installed on each finger opposes itself to the coiling process but favors the unfurling one; therefore, it is essential to ensure that the motor's shaft rotates the same angular displacement in both processes. Finally, the closing/opening processes may be interrupted and reversed if the appropriate commands are received.

B. Discrete-time $\mathcal{H}_\infty$ Feedback Controller

To design the feedback controller in charge of opening the fingers, a discretization of the simplified system is also required. Considering that the estimated state vector $\hat{\mathbf{x}}_k$ is available for feedback; that $\mathbf{x}_k \approx \hat{\mathbf{x}}_k$; and that the state information is not corrupted by the input noise $\mathbf{w}_k$, the characterization of the system is given by the Eq. 11 and the measurement equation

$$\mathbf{y}_k = \mathbf{C}\mathbf{x}_k + \mathbf{D}\mathbf{u}_k \tag{19}$$

where $\mathbf{D} \in \mathbb{R}^{q\times p}$ is the feedthrough matrix.

By choosing the following linear static state-feedback control law

$$\mathbf{u}_k = \mathbf{K}\mathbf{x}_k \tag{20}$$

where $\mathbf{K} \in \mathbb{R}^{p\times n}$ is the feedback gain that asymptotically stabilizes the closed-loop system and minimizes its $\mathcal{H}_\infty$ norm. Such a structure produces an augmented one in the following form

$$\mathbf{x}_{k+1} = \mathbf{A}_c\mathbf{x}_k + \mathbf{B}_2\mathbf{w}_k \tag{21}$$

$$\mathbf{y}_k = \mathbf{C}_c\mathbf{x}_k \tag{22}$$

with

$$\mathbf{A}_c = \mathbf{A} + \mathbf{B}_1\mathbf{K}, \quad \mathbf{B}_c = \mathbf{B}_2$$
$$\mathbf{C}_c = \mathbf{C} + \mathbf{D}\mathbf{K}$$

The goal is to find a guaranteed-cost feedback gain for the system composed by (11) and (19), which has to satisfy that $\|\mathbf{y}_k\|_2 \leq \mu\|\mathbf{w}_k\|_2$, with the robustness level $\mu \in \mathbb{R} \ni \mu > 0$. Therefore, also from the bounded-real lemma and given the transfer function $H_{wy}(z)$ for the system (21)-(22), the norm $\mathcal{H}_\infty$ can be characterized using a Lyapunov function, as follows

$$\min_{\mathbf{W},\mathbf{P}=\mathbf{P}^T>0} \mu \tag{23}$$

subjected to the following LMI

$$\begin{bmatrix} \mathbf{P} & \mathbf{A}\mathbf{P}+\mathbf{B}_1\mathbf{W} & \mathbf{0}_{n\times q} & \mathbf{B}_2 \\ \star & \mathbf{P} & \mathbf{P}\mathbf{C}^T+\mathbf{W}^T\mathbf{D}^T & \mathbf{0}_{n\times s} \\ \star & \star & \mathbf{I}_q & \mathbf{0}_{q\times s} \\ \star & \star & \star & \mu^2\mathbf{I}_s \end{bmatrix} > \mathbf{0} \tag{24}$$

where the matrices $\mathbf{W} \in \mathbb{R}^{p\times n}$ and $\mathbf{P}$ are the variables of the problem [22]. Hence, $\mathbf{K}$ can be recovered using the following expression

$$\mathbf{K} = \mathbf{W}\mathbf{P}^{-1} \tag{25}$$

Similar to the observer, one can also incorporate a slack variable, $\mathbf{G} \in \mathbb{R}^{n\times n}$, to increase the robustness of the system. This results in the following

$$\min_{\mathbf{W},\mathbf{G},\mathbf{P}=\mathbf{P}^T>0} \mu \tag{26}$$

which is subjected to

$$\begin{bmatrix} \mathbf{P} & \mathbf{A}\mathbf{G}+\mathbf{B}_1\mathbf{W} & \mathbf{0}_{n\times q} & \mathbf{B}_2 \\ \star & \mathbf{G}+\mathbf{G}^T-\mathbf{P} & \mathbf{G}^T\mathbf{C}^T+\mathbf{W}^T\mathbf{D}^T & \mathbf{0}_{n\times s} \\ \star & \star & \mathbf{I}_q & \mathbf{0}_{q\times s} \\ \star & \star & \star & \mu^2\mathbf{I}_s \end{bmatrix} > \mathbf{0} \tag{27}$$

So, $\mathbf{K}$ can be recovered by

$$\mathbf{K} = \mathbf{W}\mathbf{G}^{-1} \tag{28}$$

VI. Results

The experiments to test and validate the methods proposed throughout this work were carried out using the Galileo Hand's index finger, controlled by a customized PCB board located on the inside of the palm of the prosthetic device, with its volar side in a supine position [19], [20]. However, only the mass matrix effects were taken into account (no gravity term since most grips are in a neutral position, and no Coriolis and centripetal terms since the generalized speeds are low). Furthermore, to design both the robust $\mathcal{H}_\infty$ observer-based filter and the robust $\mathcal{H}_\infty$ feedback controller described in Sections IV and V-B, as well as to solve the convex optimization problems subjected to the LMIs described in Eqs. (14)-(16) and Eqs. (23)-(28), MATLAB, YALMIP and MOSEK were used [23], [24]. Besides, the resulting control strategy was implemented on the MCU (ARM Cortex-M4F architecture) in charge of actuating the assistive device's fingers.

The behavior of the on-off controller in tandem with the robust observer during the flexion process of the finger is shown in Fig. 4. On the upper graph, the estimation of the angular displacement of the motor shaft, $\hat{\theta}$, is juxtaposed to its ground truth alternative, θ. At the same time, the lower one represents the armature current measured by the motor driver. This estimation was established based on the data gathered by measurements acquired using a quadrature encoder for the ground truth and the on-chip ADC for the current, with a sample rate of $100\ Hz$. The gearhead's shaft's angular displacement when the finger is wholly flexed is about 4.5971 rad; while its estimated value of 4.6775 rad. These measurements imply that the active tendon was coiled around $16.5\ mm$, instead of the $16.8\ mm$ estimation. A similar discrepancy occurs on the extension process, where that error is minimal, approximately $7.2 \times 10^{-3}\ mm$.

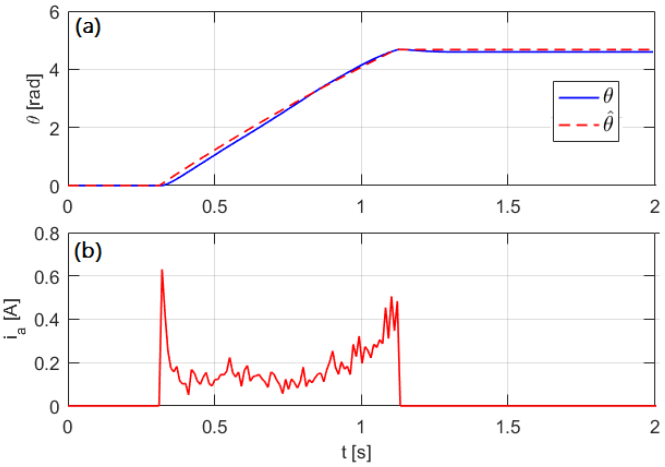

Fig. 4. (a) Motor gearhead shaft's angular displacement, θ. The dotted red line represents the estimation $\hat{\theta}$; while the solid blue line, the ground truth. (b) Current measured on the motor's armature, i_a.

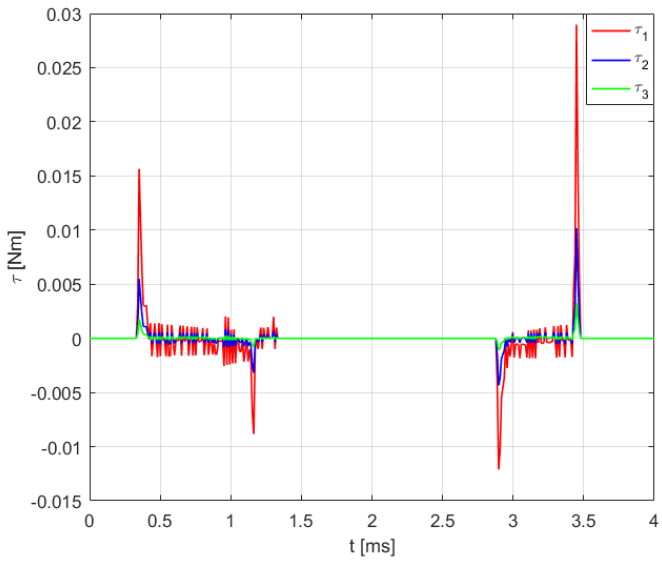

Fig. 5. Torque $\boldsymbol{\tau}$ applied on the MCP, PIP and DIP joints' axes (τ_1, τ_2 and τ_3, correspondingly).

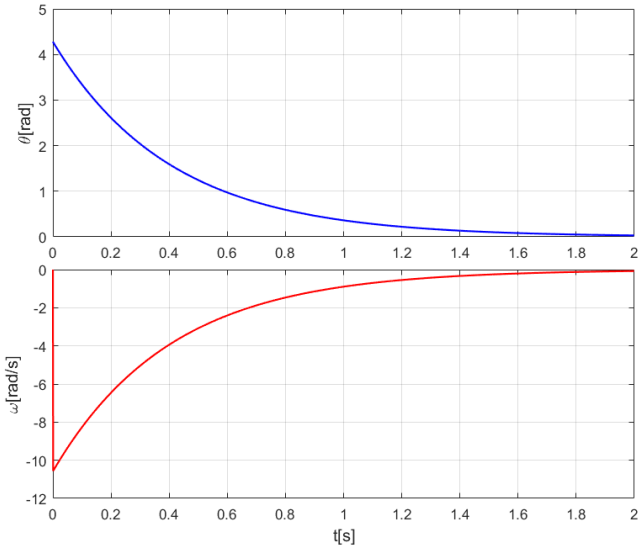

Fig. 7. The response of the robust controller during the extension process. Angular displacement and velocity, in the red and blue line, respectively.

So, this results in a root mean square error for θ of about 0.1394 rad and a robustness level, γ, of 2.2915×10^{-6}, as already shown in previous work [18]. As shown in the figure, the controller detected contact with the surface of the object at approximately 1.16 seconds, exactly when the motor stopped driving the finger.

Using the results as mentioned previously for $\hat{\theta}$, one can estimate the values of the generalized coordinates $\hat{\mathbf{q}}$ and then determine the resulting torque on each of the joints' axes, as well as the force exerted by the fingertip $\boldsymbol{f}_{tip}$. This can be visualized in Figs. 5, and 6, where the torques exerted on the MCP, PIP, and DIP joints correspond to τ_1, τ_2 and τ_3, accordingly; as well as the magnitude of fingertip force with its components on x and y directions. Besides, the behavior of the robust feedback controller described in Sec. V-B is shown in Fig. 7. As can be seen, it takes the controller about 2 seconds to complete the extension process that drives back the finger. The measurements of angular displacement and velocity, $\omega = \dot{\theta}$, were taken using the quadrature encoder specially attached for this purpose on these experiments. Finally, Fig. 8 shows active and passive tensile forces exerted during both processes.

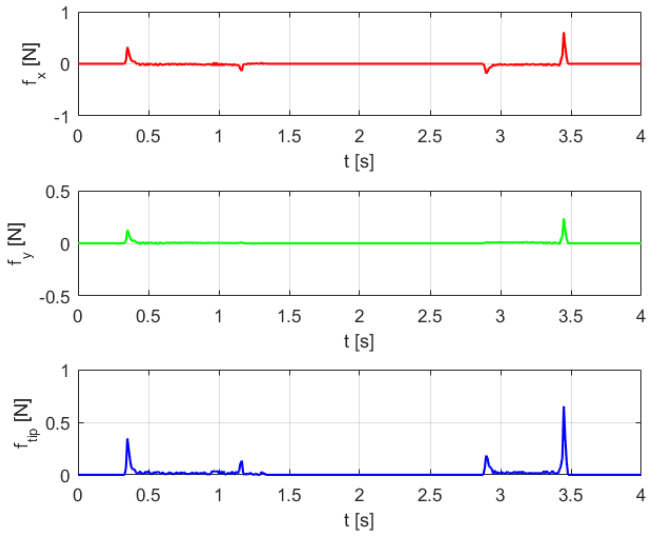

Fig. 6. Fingertip force $\boldsymbol{f}_{tip}$ exerted by the finger in x (red) and y (green) directions, as well as the magnitude of the resultant force (blue).

VII. Conclusions

In this work, a simplified dynamic model of the finger, together with the design of a hybrid robust control strategy in tandem with a robust $\mathcal{H}_\infty$ observer-based filter to estimate relevant parameters like angular displacement and the fingertip force, has proven to be a successful alternative to installing complex arrays of sensors to control affordable prostheses for transradial amputees. Additionally, these methodologies based on LMIs allow the design and use of more robust controls. They can better handle the system's disturbances since they do not make any assumptions about noise characteristics. The main drawback is the high computational power required to solve these optimization problems. However, approximating the finger dynamics to a linear system allows solving the optimization problems on a computer capable of running MATLAB and then utilizing those results to its implementation in an MCU, allowing for a more compact and affordable option to install on prosthetic devices. Since artificial hands' purpose is to determine if selected fingers are fully closed, opened, or grasping an object, rather than a precise position and orientation of the fingertips, the estimation error obtained is sufficient for ADLs' apt fulfillment. Most of the limb-impaired prefer

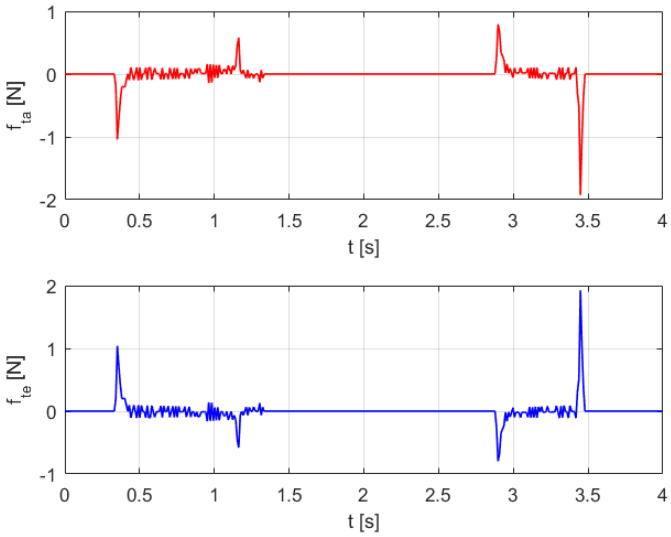

Fig. 8. Active and passive tensile forces exerted during the process, in the red and blue line, respectively.

basic functionalities such as holding a bottle, book or glass, rather than performing complicated tasks such as writing or manipulating objects with their fingers. In those cases, they prefer to use their healthy limb, if that is the case. This reinforces the idea that better and more robust controllers are necessary for the user to feel confident using this type of assistive device. Another relevant aspect is the robustness; despite the disturbances presented in the current measurement, the methods proposed in this work behave as expected, reducing noise effects on estimation and the effects that other disturbances may have on the feedback controller.

Additionally, this strategy was used to determine the kinematics and dynamics of each finger of any particular assistive device such as the Galileo Hand, as shown in Figs. 5, 6 and 8. This can be improved by designing a robust, full-order filter based on LMI methods, guaranteeing a lower robustness level, as it was presented in [25]. Finally, it is interesting to explore other possibilities by employing these methodologies in more sophisticated controllers, such as torque, impedance, and gravity compensation controllers taking into account the complexity that underactuated mechanisms as the UTD machines provide.

REFERENCES

[1] E. A. Biddiss and T. T. Chau, "Upper limb prosthesis use and abandonment: a survey of the last 25 years," *Prosthetics and orthotics international*, vol. 31, no. 3, pp. 236–257, 2007.

[2] S. Fani, M. Bianchi, S. Jain, J. S. Pimenta Neto, S. Boege, G. Grioli, A. Bicchi, and M. Santello, "Assessment of myoelectric controller performance and kinematic behavior of a novel soft synergy-inspired robotic hand for prosthetic applications," *Frontiers in neurorobotics*, vol. 10, p. 11, 2016.

[3] E. D. Engeberg, S. G. Meek, and M. A. Minor, "Hybrid force-velocity sliding mode control of a prosthetic hand," *IEEE Transactions on Biomedical Engineering*, vol. 55, no. 5, pp. 1572–1581, 2008.

[4] A. Cranny, D. Cotton, P. Chappell, S. Beeby, and N. White, "Thick-film force, slip and temperature sensors for a prosthetic hand," *Measurement Science and Technology*, vol. 16, no. 4, p. 931, 2005.

[5] C. Cipriani, M. Controzzi, and M. C. Carrozza, "The SmartHand transradial prosthesis," *Journal of neuroengineering and rehabilitation*, vol. 8, no. 1, p. 29, 2011.

[6] A. Akhtar, K. Y. Choi, M. Fatina, J. Cornman, E. Wu, J. Sombeck, C. Yim, P. Slade, J. Lee, J. Moore *et al.*, "A low-cost, open-source, compliant hand for enabling sensorimotor control for people with transradial amputations," in *2016 38th Annual International Conference of the IEEE Engineering in Medicine and Biology Society (EMBC)*. IEEE, 2016, pp. 4642–4645.

[7] L. Jiang, B. Zeng, S. Fan, K. Sun, T. Zhang, and H. Liu, "A modular multisensory prosthetic hand," in *2014 IEEE International Conference on Information and Automation (ICIA)*. IEEE, 2014, pp. 648–653.

[8] J.-K. Seok, "Frequency-spectrum-based antiwindup compensator for pi-controlled systems," *IEEE Transactions on Industrial Electronics*, vol. 53, no. 6, pp. 1781–1790, 2006.

[9] E. National Academies of Sciences, Medicine *et al.*, *The promise of assistive technology to enhance activity and work participation*. National Academies Press, 2017.

[10] E. Vazquez-Sanchez, J. Sottile, and J. Gomez-Gil, "A novel method for sensorless speed detection of brushed dc motors," *Applied Sciences*, vol. 7, no. 1, p. 14, 2017.

[11] G. C. Sincero, J. Cros, and P. Viarouge, "Arc models for simulation of brush motor commutations," *IEEE transactions on magnetics*, vol. 44, no. 6, pp. 1518–1521, 2008.

[12] T. Figarella and M. Jansen, "Brush wear detection by continuous wavelet transform," *Mechanical systems and signal processing*, vol. 21, no. 3, pp. 1212–1222, 2007.

[13] S. Yachiangkam, C. Prapanavarat, U. Yungyuen, and S. Po-ngam, "Speed-sensorless separately excited dc motor drive with an adaptive observer," in *2004 IEEE Region 10 Conference TENCON 2004.*, vol. 500. IEEE, 2004, pp. 163–166.

[14] S. R. Bowes, A. Sevinc, and D. Holliday, "New natural observer applied to speed-sensorless dc servo and induction motors," *IEEE transactions on industrial electronics*, vol. 51, no. 5, pp. 1025–1032, 2004.

[15] S. Praesomboon, S. Athaphaisal, S. Yimman, R. Boontawan, and K. Dejhan, "Sensorless speed control of dc servo motor using kalman filter," in *2009 7th International Conference on Information, Communications and Signal Processing (ICICS)*. IEEE, 2009, pp. 1–5.

[16] A. Khalid and A. Nawaz, "Sensor less control of dc motor using kalman filter for low cost cnc machine," in *2014 International Conference on Robotics and Emerging Allied Technologies in Engineering (iCREATE)*. IEEE, 2014, pp. 180–185.

[17] O. Aydogmus and M. F. Talu, "Comparison of extended-kalman-and particle-filter-based sensorless speed control," *IEEE Transactions on Instrumentation and Measurement*, vol. 61, no. 2, pp. 402–410, 2011.

[18] J. Fajardo, D. Cardona, G. Maldonado, A. R. Neto, and E. Rohmer, "A robust H_∞ full-state observer for under-tendon-driven prosthetic hands," in *2020 IEEE/ASME International Conference on Advanced Intelligent Mechatronics (AIM)*. IEEE, 2020, pp. 1555–1560.

[19] J. Fajardo, V. Ferman, A. Lemus, and E. Rohmer, "An affordable open-source multifunctional upper-limb prosthesis with intrinsic actuation," in *2017 IEEE Workshop on Advanced Robotics and its Social Impacts (ARSO)*. IEEE, 2017, pp. 1–6.

[20] J. Fajardo, V. Ferman, D. Cardona, G. Maldonado, A. Lemus, and E. Rohmer, "Galileo hand: An anthropomorphic and affordable upper-limb prosthesis," *IEEE Access*, vol. 8, pp. 81 365–81 377, 2020.

[21] R. Ozawa, K. Hashirii, and H. Kobayashi, "Design and control of underactuated tendon-driven mechanisms," in *2009 IEEE International Conference on Robotics and Automation*. IEEE, 2009, pp. 1522–1527.

[22] M. C. De Oliveira, J. C. Geromel, and J. Bernussou, "Extended H_2 and H_∞ norm characterizations and controller parametrizations for discrete-time systems," *International Journal of Control*, vol. 75, no. 9, pp. 666–679, 2002.

[23] M. ApS, "The MOSEK optimization toolbox for MATLAB," *User's Guide and Reference Manual, version*, vol. 4, 2019.

[24] J. Lofberg, "YALMIP: A toolbox for modeling and optimization in MATLAB," in *2004 IEEE international conference on robotics and automation (IEEE Cat. No. 04CH37508)*. IEEE, 2004, pp. 284–289.

[25] J. C. Geromel, J. Bernussou, G. Garcia, and M. C. de Oliveira, "H_2 and H_∞ robust filtering for discrete-time linear systems," *SIAM Journal on Control and Optimization*, vol. 38, no. 5, pp. 1353–1368, 2000.